

# Impact of lesion morphology on stent elongation during bifurcation PCI: an *in vivo* OCT study

Michael McGarvey<sup>1,2</sup>, MA, MBBS; Lap-Tin Lam<sup>1</sup>, MD; Muhamad Abd Razak<sup>1,2</sup>, MBBS; Jennifer Barraclough<sup>3</sup>, MBBS, PhD; Kevin O’Gallagher<sup>1,2</sup>, MA, PhD; Ian Webb<sup>1</sup>, MA, PhD; Narbeh Melikian<sup>1,2</sup>, BSc, MD; Sundeep Kalra<sup>4</sup>, PhD; Philip MacCarthy<sup>1,2</sup>, BSc, PhD; Ajay M. Shah<sup>1,2</sup>, MD; Jonathan M. Hill<sup>5</sup>, MD; Thomas W. Johnson<sup>3</sup>, BSc, MBBS, MD; Jonathan Byrne<sup>1,2</sup>, BSc, PhD; Rafal Dworakowski<sup>1,2</sup>, PhD; Nilesh Pareek<sup>1,2\*</sup>, MA, PhD

\*Corresponding author: School of Cardiovascular and Metabolic Medicine and Sciences, BHF Centre of Excellence, Level 3, James Black Centre, Denmark Hill Campus, King’s College London, London, SE5 9NU, United Kingdom. E-mail: [nileshpareek@nhs.net](mailto:nileshpareek@nhs.net)

## ABSTRACT

**BACKGROUND:** Recent observations *in silico* and *in vivo* reported that, during proximal optimisation technique, drug-eluting stents (DES) elongate, challenging conventional wisdom. The interaction between plaque morphology and radial expansion is well established, but little is known about the impact of plaque morphology on elongation.

**AIMS:** We aimed to assess the longitudinal mechanical behaviour of contemporary DES *in vivo* and evaluate the relationship between post-percutaneous coronary intervention (PCI) stent elongation and lesion morphology, as assessed with optical coherence tomography (OCT).

**METHODS:** Patients treated with OCT-guided PCI to left main or left anterior descending artery bifurcations, between July 2017 and March 2022, from the King’s Optical coherence Database Analysis Compendium were included. Patients were excluded if there were overlapping stents, if they had undergone prior PCI, or if there was inadequate image quality. Lesions were characterised as fibrocalcific, fibrous or lipid-rich by pre-PCI OCT. Following stent post-dilatation, stent expansion and final stent length were assessed. The primary outcome was the percentage change in stent length from baseline.

**RESULTS:** Of 501 eligible consecutive patients from this period, 116 were included. The median age was 66 years (interquartile range [IQR] 57-76), 31% were female, and 53.4% were treated for an acute coronary syndrome. A total of 50.0% of lesions were classified as fibrocalcific, 6.9% were fibrous, and 43.1% were lipid-rich. The change in relative stent length was 4.4% (IQR 1.0-8.9), with an increase of 3.1% (IQR 0.5-6.3) in fibrocalcific lesions, 3.3% (IQR 0.5-5.9) in fibrous lesions, and 6.4% (IQR 3.1-11.1) in lipid-rich plaque ( $p=0.006$ ). In multivariate regression modelling, lipid-rich plaque was an independent predictor of stent elongation (odds ratio 3.689, 95% confidence interval: 1.604-8.484).

**CONCLUSIONS:** Contemporary DES elongate following implantation and post-dilatation, and this is significantly mediated by plaque morphology. This is an important consideration when planning a strategy for DES implantation.

**KEYWORDS:** OCT; plaque morphology; stent elongation

Coronary artery disease (CAD) is the most common cause of death globally and is routinely treated with drug-eluting stents (DES), in stable and acute settings<sup>1,2</sup>. Contemporary second- and third-generation DES are characterised by thin (or ultrathin) struts and sophisticated platform designs that provide excellent deliverability and high radial strength, with low rates of thrombosis and restenosis<sup>3</sup>. Understanding the biomechanical properties of contemporary DES *in vivo* is critical to ensure their appropriate and effective use, particularly in the treatment of bifurcation lesions. The expansion capacities and radial mechanical strength of contemporary DES have been extensively studied, but less is known about the longitudinal mechanical properties of contemporary platforms and how this affects *in vivo* behaviour<sup>4,5</sup>.

Conventional wisdom, based on early observations of self-expanding stents, proposed that stents shorten during overexpansion and proximal optimisation technique (POT)<sup>6</sup>. However, recent analyses from *in silico* models and *in vivo* assessment with optical coherence tomography (OCT) have challenged this paradigm. In these studies, the performance of POT was associated with proximal elongation of the DES<sup>7-9</sup>. Although the number of patients in these studies was small, the clinical repercussions may be highly significant – unpredictable longitudinal stent behaviour may lead to ostial stent protrusion, unintentional side branch coverage, major stent malapposition and proximal underexpansion, potentially increasing the risk of stent failure<sup>3,10</sup>.

Plaque morphology, which is assessed with intracoronary (IC) imaging, influences percutaneous coronary intervention (PCI) technique and may predict a stent's mechanical behaviour *in vivo*. The interaction of plaque morphology and radial expansion is well described, but the relationship between plaque morphology and longitudinal mechanical behaviour *in vivo* is unclear<sup>11</sup>. An improved understanding of the *in vivo* longitudinal properties of DES, the factors that influence elongation, and how we may minimise associated adverse sequelae is required.

Accordingly, the purpose of this study was to describe the extent of stent elongation in a large real-world cohort and to evaluate the relationship between pre-PCI plaque morphology and longitudinal stent behaviour during coronary bifurcation PCI.

Editorial, see page e1127

## Methods

### STUDY SETTING

The King's Optical coherence Database Analysis Compendium (KODAC) is a single-centre, retrospective registry of 1,838 consecutive patients who underwent invasive assessment with

### Impact on daily practice

Iterative developments in drug-eluting stent (DES) technology have produced devices that are highly deliverable, with excellent radial strength and expansion capacities. This has come at the expense of longitudinal strength. We demonstrate that contemporary DES can elongate by up to 11.1% in lipid-rich plaque. This may result in ostial stent protrusion, accidental “jailing” of clinically important side branch ostia, stent underexpansion and major malapposition. Clinicians must consider these intrinsic features of contemporary DES platforms and their interaction with plaque morphology to ensure precise and durable results for patients treated by percutaneous coronary intervention. Device technology must evolve to improve the predictability of longitudinal performance.

IC OCT at King's College Hospital between March 2013 and March 2022. King's College Hospital is a large, tertiary cardiac centre, serving a population of approximately two million people in central London, United Kingdom. Cases in the KODAC Registry include patients with stable angina and those admitted with acute coronary syndromes, including emergency primary PCI for ST-segment elevation myocardial infarction (STEMI). Indications for OCT assessment and its utilisation remained at the treating clinician's discretion.

### STUDY POPULATION AND DATA COLLECTION

Patients treated with second- or third-generation DES for *de novo* atherosclerotic bifurcation lesions were included. To ensure the use of contemporary DES platforms, we restricted analysis to procedures performed between 1 July 2017 and 31 March 2022, identifying consecutive adult patients with paired pre- and post-PCI OCT assessment. To minimise any effect from vessel tortuosity or curvature, only patients treated with PCI to bifurcation lesions in the left main stem (LMS) and/or left anterior descending artery (LAD) were included. Bifurcation lesions were defined as a 50% coronary stenosis adjacent to and/or involving an adequate-sized side branch (SB;  $\geq 2.0$  mm in reference diameter), with the lesion located  $\leq 4$  mm from the point of bifurcation, as assessed by angiography. These definitions are in accordance with recent consensus from the Bifurcation Academic Research Consortium<sup>12</sup>.

Patients were excluded if one or more of the following criteria were met: (1) prior PCI had been performed in the region of interest; (2) images were of insufficient quality to allow accurate interpretation (i.e., entire stent length was

### Abbreviations

<b>CoCr-EES</b>	cobalt-chromium everolimus-eluting stent	<b>KODAC</b>	King's Optical coherence Database Analysis Compendium	<b>PCI</b>	percutaneous coronary intervention
<b>CoCr-SES</b>	cobalt-chromium sirolimus-eluting stent	<b>LAD</b>	left anterior descending artery	<b>POT</b>	proximal optimisation technique
<b>CoNi-ZES</b>	cobalt-nickel zotarolimus-eluting stent	<b>LMS</b>	left main stem	<b>PtCr-EES</b>	platinum-chromium everolimus-eluting stent
<b>DES</b>	drug-eluting stent	<b>MSA</b>	minimum stent area	<b>SEI</b>	stent expansion index
<b>IC</b>	intracoronary	<b>OCT</b>	optical coherence tomography	<b>STEMI</b>	ST-segment elevation myocardial infarction

not captured in a single OCT run, or successive images in the region of interest had >1 quartile obscured by artefact or thrombus); (3) overlapping stents were present (including those treated with a culotte or “inverted culotte” technique) – two-stent techniques that did not involve longitudinal stent overlap in the main branch were included (e.g., double-kissing [DK] crush or T/T and small protrusion [T/TAP]).

Baseline characteristics were collected from medical records and from the British Cardiovascular Intervention Society (BCIS) audit database, including age, sex, clinical syndrome and cardiovascular risk factors<sup>13</sup>.

### IMAGE ANALYSIS & PROCEDURAL DATA

OCT images were acquired using a frequency domain OCT system (Abbott) and submitted to the KODAC Registry. Lesions were categorised as fibrocalcific, fibrous, or lipid-rich, based on pre-PCI assessment with OCT. In accordance with established criteria, fibrous plaques were defined as homogeneous, signal-rich lesions. Lipid pools appear as signal-poor regions with a diffuse border and overlying signal-rich bands (fibrous caps), with high signal attenuation. Where the lipid arc extends beyond 90°, the lesion was defined as lipid-rich. Calcified plaques are signal-poor regions with sharply delineated borders and limited shadowing, with calcified nodules defined as single or multiple regions of calcium that protrude into the lumen. Thin-cap fibroatheromas were defined as lipid-rich lesions with a minimum fibrous cap thickness  $\leq 65 \mu\text{m}$ <sup>14</sup>. A fibrous cap was identified as a signal-rich band overlying the lipid core. The minimum fibrous cap thickness was measured 3 times at its thinnest part, and the average value was recorded<sup>15</sup>.

In stenoses where more than one morphology was present, lesions were categorised based on a qualitative assessment of the predominant morphology at the site of the minimum lumen area (and frames 2 mm either side). The OCT images were independently assessed by two interventional cardiologists (M. McGarvey and L.-T. Lam), and in the case of discrepancy, a third interventional cardiologist (N. Pareek) adjudicated. Validation of the reliability of this method was provided by an independent expert in IC imaging (T.W. Johnson).

Stent inflow and outflow were defined as the proximal and distal frames where stent struts occupied  $\geq 180^\circ$  of a vessel circumference on OCT. Post-PCI stent length was the distance measured between these points on the longitudinal view. Minimum stent area (MSA) and relative stent expansion (defined as the MSA divided by the mean of the proximal and distal reference areas) was recorded<sup>16</sup>. We sought to assess the importance of proximal and distal stent expansion using criteria set out in the ILUMIEN IV: OPTIMAL PCI trial protocol. Briefly, the stent was divided in two, either into equal segments or at the site of bifurcation (i.e., side branch  $\geq 2.0$  mm diameter). The MSA in the proximal and distal segments were defined relative to the proximal and distal reference values, respectively<sup>17</sup>. Finally, we evaluated the stent expansion index (SEI), a modified form of the ILUMIEN protocol. SEI requires the identification of the MSA in each half of the divided stent, along with the proximal and distal reference values in each stent segment.

Relative stent expansion was calculated in each segment, with the smaller value representing the SEI<sup>18</sup>.

The stent manufacturer and platform, index stent length and diameter, and POT balloon diameter were extracted from procedural reports. The nominal size of the POT balloon was taken as the diameter, and this was not adjusted to pressure-diameter charts.

### OUTCOMES

The primary outcome measure in this study is the percentage change in stent length from baseline after performance of post-dilatation and POT. Secondary outcomes include the absolute change in stent length from baseline and markers of post-PCI stent expansion including the MSA, relative stent expansion, proximal and distal segment stent expansion, and the SEI.

### STATISTICAL ANALYSIS

Baseline patient, lesion and procedural characteristics are presented as frequencies or mean  $\pm$  standard deviation for normally distributed variables, and as medians with interquartile range (IQR) for non-normally distributed data. The Shapiro-Wilks test of normality was applied to all continuous variables. Between-group comparisons were performed with the chi-square test for proportions; one-way analysis of variance (ANOVA) was used for continuous, normally distributed variables (with Tukey’s *post hoc* test for paired comparisons between groups); and the Kruskal-Wallis one-way ANOVA was performed for comparison of non-normally distributed variables.

Logistic regression analysis was used to assess if key lesion and procedural characteristics predicted a greater than median percentage stent elongation *in vivo*. Greater than median stent elongation was chosen as the outcome to avoid imbalance in the regression model<sup>19</sup>. Continuous variables were not categorised or dichotomised to optimise power in the regression model<sup>20</sup>. We performed exploratory univariable logistic regression to identify candidate variables that may be associated with a greater than median percentage stent elongation in this population. Results are presented as odds ratios (OR) with 95% confidence intervals (CI). Variables that were found to be statistically significant in relation to a greater than median percentage stent elongation were entered into a multivariable logistic regression model to identify independent predictors of a greater than median percentage elongation.

A  $p$ -value  $< 0.05$  was considered statistically significant, with a Bonferroni correction for the adjustment of  $p$ -value for the paired comparison of subgroups. Analyses were performed with SPSS Statistics, version 29.0.2.0 (IBM) and Prism, version 9.0 (GraphPad Software).

### ETHICS & ROLE OF THE FUNDING SOURCE

This project operated under the Health and Social Care Research Ethics Committee B approval (reference 23/NI/0077) granted to the King’s College London Cardiovascular Diseases Database (KCL-CVD). The funders had no role in study design, data collection and analysis, decision to publish, or preparation of the manuscript. The study was performed according to the principles of the Declaration of Helsinki.

## Results

Between 1 July 2017 and 30 March 2022, 501 consecutive patients in the KODAC Registry underwent OCT-guided PCI of the left main and/or LAD coronary arteries. A total of 116 were deemed eligible for inclusion in this study. We excluded 231 patients due to treatment with overlapping stents, 58 patients underwent DES PCI for in-stent restenosis, and 24 patients were treated with “plain old balloon” or drug-coated balloon angioplasty only. A further 46 patients were excluded, as no pre-PCI OCT assessment was performed, and in 18 patients, inadequate OCT image quality precluded accurate classification of plaque morphology or assessment of post-PCI stent length and expansion. In addition, 8 patients had lesions that did not satisfy the definition of a bifurcation and were excluded (**Figure 1**).

The median age of the patients was 66 years (IQR 57-76), and 31.0% (n=36/116) were female. In total, 53.4% (n=62/116) patients were treated following an acute coronary syndrome, and 23.7% (n=27/114) had a history of myocardial infarction. Type 2 diabetes mellitus was present in 33.0% (n=37/112) of patients, 58.6% (n=68/116) had hypertension, and 5.3% (n=6/113) had chronic kidney disease (**Table 1**). A total of 58 (50.0%) lesions were classified as fibrocalcific, 8 (6.9%) as fibrous, and 50 (43.1%) as lipid-rich. A sample of 43 baseline OCTs were assessed and categorised by an independent external OCT expert (T.W. Johnson). Assessment of the inter-rater reliability of lesion categorisation demonstrated substantial agreement, with a Cohen's  $\kappa$  statistic of 0.701<sup>21</sup>.

Fibrocalcific lesions demonstrated greater maximum calcium arc ( $p<0.001$ ), maximum calcium depth ( $p<0.001$ ), and calcium length ( $p<0.001$ ) compared to fibrous and lipid-rich plaques. In all, 53.4% (n=31/58) of fibrocalcific lesions had a calcium volume index of 4, and 37.9% (n=22/58) contained a calcified nodule. Lipid-rich lesions had thinner minimum fibrous cap thickness ( $p=0.002$ ), greater maximum lipid arc ( $p<0.001$ ) and greater lipid length ( $p<0.001$ ) (**Table 2**).

Patients with fibrocalcific lesions were older and were more likely to have a history of hypercholesterolaemia and diabetes mellitus. Baseline angiographic and procedural characteristics were otherwise similar (**Table 3**). True bifurcation disease (i.e., Medina classification 1,1,1 or 1,0,1 or 0,1,1)<sup>12</sup> was evident in 26.7% (n=31/116) of cases, with 31.9% (n=37/116) of lesions involving the LMS bifurcation. LAD/first diagonal bifurcations were treated in 57.8% of cases (n=67/116), with a further 10.3% of cases (n=12/116) involving the LAD/second diagonal bifurcation.

XIENCE cobalt-chromium everolimus-eluting stents (CoCr-EES [Abbott]) were used for the majority of procedures (n=78/116, 67.2%). A total of 25/116 patients (21.6%) were treated with SYNERGY platinum-chromium (PtCr)-EES (Boston Scientific), 7/116 (6.0%) with Promus PREMIER PtCr-EES (Boston Scientific), 4/116 (3.4%) with Resolute Onyx cobalt-nickel zotarolimus-eluting stents (CoNi-ZES [Medtronic]), and 2/116 patients (1.7%) were treated with Orsiro CoCr sirolimus-eluting stents (SES [Biotronik]).

The nominal baseline stent length was 28.0 mm (IQR 23.0-38.0), and the nominal baseline stent diameter was 3.0 mm (IQR 2.75-3.50). Proximal optimisation or post-dilatation was performed in all cases. The maximum median

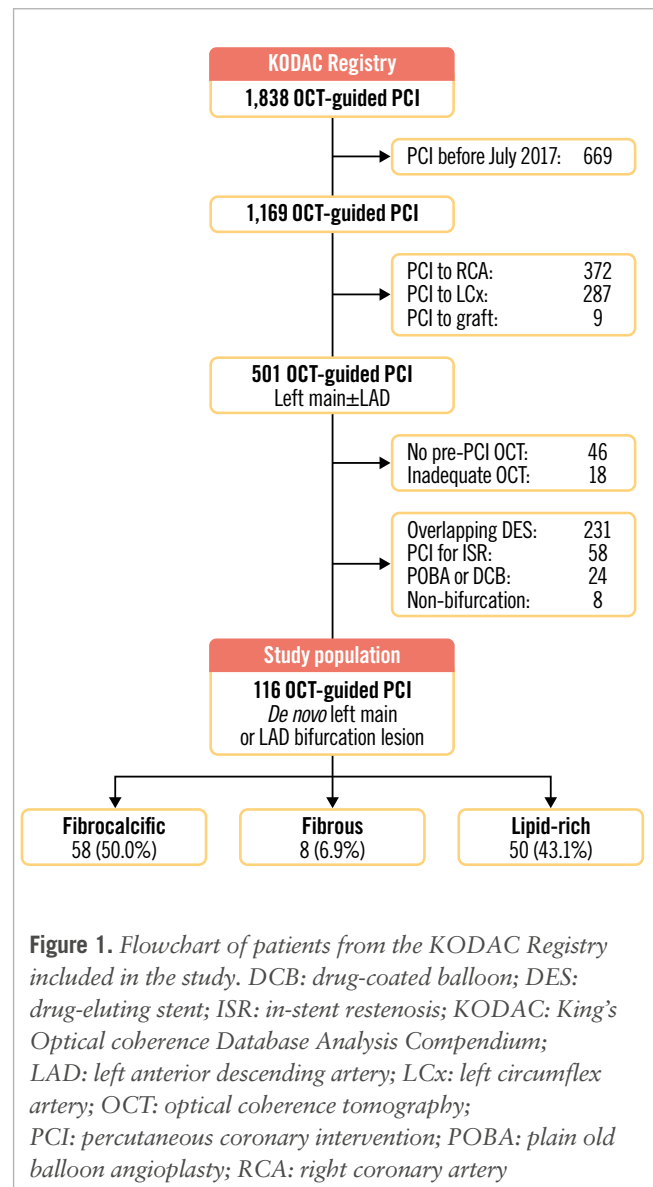


**Figure 1.** Flowchart of patients from the KODAC Registry included in the study. DCB: drug-coated balloon; DES: drug-eluting stent; ISR: in-stent restenosis; KODAC: King's Optical coherence Database Analysis Compendium; LAD: left anterior descending artery; LCx: left circumflex artery; OCT: optical coherence tomography; PCI: percutaneous coronary intervention; POBA: plain old balloon angioplasty; RCA: right coronary artery

post-dilatation balloon diameter was 3.75 mm (IQR 3.5-4.0), with a median POT balloon overexpansion of 117% (IQR 113-133), relative to the nominal stent diameter.

## OUTCOMES

Post-PCI OCT demonstrated a median relative stent elongation of 4.4% (IQR 1.0-8.9) and absolute elongation of 1.3 mm (IQR 0.3-2.2) from the nominal baseline length (**Figure 2**). There was a significant increase in stent length following implantation and post-dilatation, from a nominal baseline length of 28.0 mm (IQR 23.0-38.0) to 31.1 mm (IQR 23.9-38.2;  $p<0.001$ ).

Post-PCI stent elongation differed significantly according to the underlying lesion morphology ( $p=0.006$ ). Relative stent elongation in fibrocalcific lesions was 3.1% (IQR 0.5-6.3). Lipid-rich lesions facilitated the greatest change in relative stent length, with an increase of 6.4% (IQR 3.1-11.1) – this was significantly greater than the elongation observed in fibrocalcific lesions ( $p=0.006$ ) but not in fibrous lesions ( $p=0.354$ ) (**Table 4**).

**Table 1. Baseline patient characteristics.**

	Total population (N=116)	Fibrocalcific plaque (N=58)	Fibrous plaque (N=8)	Lipid-rich plaque (N=50)	p-value
Age, years	66 (57-76)	73 (63-79)	65 (60-69)	58 (50-69)	<b>&lt;0.001</b>
Female	36/116 (31)	18/58 (31)	3/8 (37.5)	15/50 (30)	0.913
ACS	62/116 (53.4)	28/58 (48.3)	4/8 (50.0)	30/50 (60.0)	0.467
Hypertension	68/116 (58.6)	38/58 (65.5)	5/8 (62.5)	25/50 (50.0)	0.257
Hypercholesterolaemia	46/116 (39.7)	29/50 (50.0)	4/8 (50.0)	13/50 (26.0)	<b>0.033</b>
Previous MI	27/114 (23.7)	18/56 (32.1)	0/8 (0)	9/50 (18.0)	0.061
Diabetes mellitus	37/112 (33.0)	25/57 (43.9)	3/8 (37.5)	9/47 (19.1)	<b>0.027</b>
Stroke/TIA	3/116 (2.6)	1/58 (1.7)	0/8 (0)	2/50 (4.0)	0.677
Chronic kidney disease (Creatinine >200 µmol or HDx)	6/113 (5.3)	3/55 (5.4)	2/8 (25)	1/50 (2.0)	<b>0.008</b>
Current smoker	15/98 (15.3)	5/47 (10.6)	0/7 (0)	10/44 (22.7)	0.141

Values are median (IQR), or n/N (%). P-values in bold indicate statistical significance. Proportions were compared using chi-square tests. Medians were compared using the Kruskal-Wallis one-way ANOVA. ACS: acute coronary syndrome; ANOVA: analysis of variance; HDx: expanded haemodialysis; IQR: interquartile range; MI: myocardial infarction; TIA: transient ischaemic attack

**Table 2. Optical coherence tomography assessment of lesion characteristics.**

	Total population (N=116)	Fibrocalcific plaque (N=58)	Fibrous plaque (N=8)	Lipid-rich plaque (N=50)	p-value
<b>Lesion dimensions</b>					
Minimum lumen area, mm <sup>2</sup>	2.42 (1.90-3.02)	2.45 (1.81-3.14)	3.19 (2.39-3.94)	2.26 (1.95-2.90)	0.116
Proximal reference diameter, mm	3.90 (3.60-4.24)	3.90 (3.53-4.20)	3.79 (3.37-4.28)	3.94 (3.75-4.39)	0.269
Distal reference diameter, mm	3.11 (2.86-3.02)	3.10 (2.80-3.50)	2.98 (2.49-3.38)	3.15 (2.92-3.68)	0.216
Proximal reference area: MLA ratio	4.43 (3.34-5.83)	3.92 (2.99-5.52)	2.92 (2.29-5.49)	4.65 (4.02-6.20)	<b>0.019</b>
<b>Morphological characteristics</b>					
Maximum lipid arc, °	150.5 (96.7-150.5)	124.0 (88.0-166.9)	79.6 (15.0-84.6)	200.5 (139.8-265.3)	<b>&lt;0.001</b>
Lipid length, mm	6.20 (2.90-10.90)	3.40 (2.15-6.20)	4.20 (0.75-7.50)	10.85 (8.38-13.25)	<b>&lt;0.001</b>
Minimum fibrous cap thickness, µm	110 (85.3-150.0)	127.5 (98.8-166.3)	165.0 (102.5-327.5)	101.5 (75.0-130)	<b>0.002</b>
Thin-cap fibroatheroma	11/116 (9.5)	1/58 (1.7)	0/8 (0.0)	10/50 (20.0)	<b>0.003</b>
Calcium morphology					<b>&lt;0.001</b>
No calcium	31/116 (26.7)	0/58 (0.0)	5/8 (62.5)	26/50 (52.0)	
Sheet calcium only	60/116 (51.7)	36/58 (60.0)	3/8 (37.5)	21/50 (42.0)	
Concentric calcium	7/116 (6.0)	7/58 (12.1)	0/8 (0.0)	0/50 (0.0)	
Calcified nodule	25/116 (21.6)	22/58 (37.9)	0/8 (0.0)	3/50 (6.0)	
Maximum calcium arc, °	111.5 (0.0-197.8)	186 (130.3-257.4)	0 (0.0-64.4)	0 (0.0-99.3)	<b>&lt;0.001</b>
Maximum calcium depth, mm	0.77 (0.00-1.04)	0.99 (0.82-1.15)	0.0 (0.0-0.44)	0.0 (0.0-0.71)	<b>&lt;0.001</b>
Calcium length, mm	4.90 (0.0-10.20)	9.20 (6.03-16.38)	0.0 (0.0-2.2)	0.0 (0.0-3.78)	<b>&lt;0.001</b>
Calcium volume index					<b>&lt;0.001</b>
0	39/116 (33.6)	1/58 (1.7)	7/8 (87.5)	31/50 (62.0)	
1	20/116 (17.2)	8/58 (6.9)	1/8 (12.5)	11/50 (22.0)	
2	21/116 (18.1)	16/58 (27.6)	0/8 (0.0)	5/50 (10.0)	
3	2/116 (1.7)	2/58 (3.4)	0/8 (0.0)	0/50 (0.0)	
4	34/116 (29.3)	31/58 (53.4)	0/8 (0.0)	3/50 (6.0)	

Values are median (IQR), or n/N (%). P-values in bold indicate statistical significance. Proportions were compared using chi-square tests. Medians were compared using the Kruskal-Wallis one-way ANOVA. ANOVA: analysis of variance; IQR: interquartile range; MLA: minimum lumen area

**Table 3. Angiographic and procedural characteristics.**

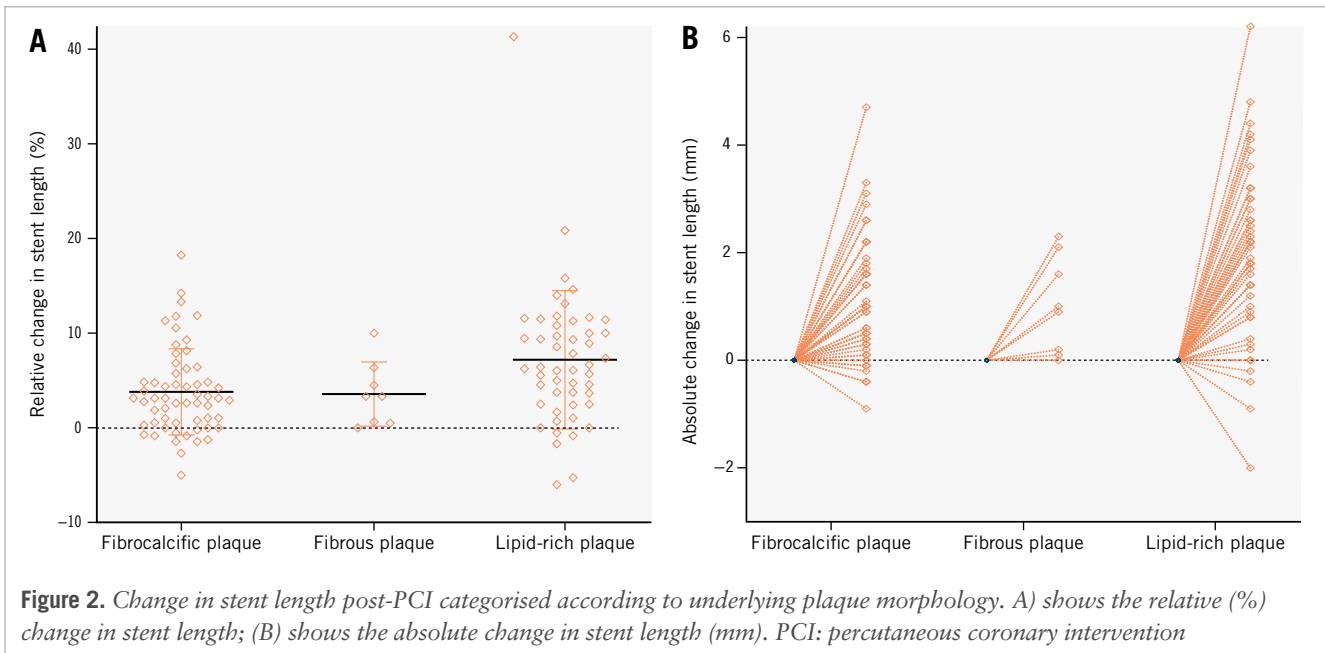
	Total population (N=116)	Fibrocalcific plaque (N=58)	Fibrous plaque (N=8)	Lipid-rich plaque (N=50)	p-value
<b>Angiographic characteristics</b>					
“True” bifurcation (Medina 1,1,1/1,0,1/0,1,1)	31/116 (26.7)	19/58 (32.8)	0/8 (0)	12/50 (24.0)	0.123
Left main bifurcations	37/116 (31.9)	18/58 (31.0)	1/8 (12.5)	18/50 (36.0)	0.408
LAD/diagonal 1	67/116 (57.8)	34/58 (58.6)	6/8 (75.0)	27/50 (54.0)	0.527
LAD/diagonal 2	12/116 (10.3)	6/58 (10.3)	1/8 (12.5)	5/50 (10.0)	0.977
<b>Bifurcation PCI strategy</b>					
Crossover MV only	77/116 (66.4)	38/58 (65.5)	6/8 (75.0)	33/50 (66.0)	0.865
Proximal MV only	5/116 (4.3)	4/58 (6.9)	0/8 (0.0)	1/50 (2.0)	0.378
Distal MV only	28/116 (24.1)	12/58 (20.7)	2/8 (25.0)	14/50 (28.0)	0.675
DK crush	3/116 (2.6)	2/58 (3.4)	0/8 (0)	1/50 (2.0)	0.798
T/TAP	3/116 (2.6)	2/58 (3.4)	0/8 (0)	1/50 (2.0)	0.798
Final kissing inflation	5/116 (4.3)	3/58 (5.2)	0/8 (0)	2/50 (4.0)	0.788
<b>Post-dilatation &amp; POT</b>					
POT balloon diameter, mm	3.75 (3.50-4.00)	3.50 (3.50-4.00)	3.88 (3.50-4.00)	4.00 (3.50-4.13)	0.129
Post-dilatation/POT overexpansion, %	117 (113-133)	117 (113-128)	125 (104-143)	128 (114-133)	0.463
<b>Stent platform</b>					
Baseline stent diameter, mm	3.00 (2.75-3.50)	3.00 (2.75-3.50)	3.00 (2.75-3.50)	3.00 (2.94-3.50)	0.734
Baseline stent length, mm	28.0 (23.0-38.0)	32.0 (23.0-38.0)	29.0 (20.8-32.8)	28.0 (21.5-38.0)	0.457
CoCr-EES	78/116 (67.2)	39/58 (67.2)	4/8 (50.0)	35/50 (70.0)	0.535
Promus PtCr-EES <sup>1</sup>	7/116 (6.0)	2/58 (3.4)	1/8 (12.5)	4/50 (8.0)	0.446
CoNi-ZES	4/116 (3.4)	2/58 (3.4)	0/8 (0)	2/50 (4.0)	0.847
SYNERGY PtCr-EES <sup>1</sup>	25/116 (21.6)	14/58 (24.1)	2/8 (25.0)	9/50 (18.0)	0.719
CoCr-SES	2/116 (1.7)	1/58 (1.7)	1/8 (12.5)	0/50 (0)	<b>0.042</b>

Values are median (IQR), or n/N (%). P-value in bold indicates statistical significance. Proportions were compared using chi-square tests. Medians were compared using the Kruskal-Wallis one-way ANOVA. <sup>1</sup>Boston Scientific. ANOVA: analysis of variance; CoCr-EES: cobalt-chromium everolimus-eluting stent; CoCr-SES: cobalt-chromium sirolimus-eluting stent; CoNi-ZES: cobalt-nickel zotarolimus-eluting stent; DK: double kissing; LAD: left anterior descending artery; MV: main vessel; PCI: percutaneous coronary intervention; POT: proximal optimisation technique; PtCr-EES: platinum-chromium everolimus-eluting stent; T/TAP: T/T and small protrusion

**Table 4. Primary and secondary outcome measures.**

	Total population (N=116)	Fibrocalcific plaque (N=58)	Fibrous plaque (N=8)	Lipid-rich plaque (N=50)	p-value
Change in stent length from nominal, %	4.4 (1.0-8.9)	3.1 (0.5-6.3)	3.3 (0.5-5.9)	6.4 (3.1-11.1)	<b>0.006</b>
Fibrocalcific vs fibrous					1.000 <sup>a</sup>
Fibrocalcific vs lipid-rich					<b>0.006<sup>a</sup></b>
Fibrous vs lipid-rich					0.354 <sup>a</sup>
Absolute change in stent length, mm	1.3 (0.3-2.2)	1.0 (0.2-1.8)	1.0 (0.1-2.0)	1.8 (0.9-2.7)	<b>0.011</b>
Fibrocalcific vs fibrous					1.000 <sup>a</sup>
Fibrocalcific vs lipid-rich					<b>0.010<sup>a</sup></b>
Fibrous vs lipid-rich					0.434 <sup>a</sup>
<b>Stent expansion indices</b>					
Minimum stent area, mm <sup>2</sup>	5.27 (4.9-7.6)	5.5 (4.5-7.7)	5.2 (4.3-6.7)	6.2 (4.9-7.6)	0.403
Relative stent expansion, %	69.6 (60.6-79.8)	70.1 (62.5-83.5)	73.2 (49.1-80.2)	69.4 (59.8-78.9)	0.316
“Acceptable” stent expansion (≥80% relative expansion)	28/115 (24.3)	15/58 (25.9)	2/8 (25.0)	11/49 (22.4)	0.919
Proximal stent expansion, %	80.0 (68.0-90.6)	81.3 (66.0-91.7)	79.0 (62.2-96.3)	79.9 (69.4-90.0)	0.985
Distal stent expansion, %	91.5 (84.1-99.1)	90.9 (85.6-98.7)	93.7 (84.7-97.9)	91.8 (80.7-99.1)	0.827
Stent expansion index	0.77 (0.71-0.85)	0.77 (0.71-0.85)	0.80 (0.70-0.83)	0.78 (0.72-0.85)	0.912

Values are median (IQR), or n/N (%). Non-normally distributed variables are presented as median (IQR), and were compared using the Kruskal-Wallis one-way ANOVA. P-values in bold indicate statistical significance. <sup>a</sup>Paired comparisons with adjusted p-value using the Bonferroni correction. ANOVA: analysis of variance; IQR: interquartile range



Across all lesions, the median post-PCI MSA was 5.27 mm<sup>2</sup> (IQR 4.9-7.6), and relative stent expansion was 69.6% (IQR 60.6-79.8). Expansion in the distal stent segment was 91.5% (IQR 84.1-99.1) and 80.0% (IQR 68.0-90.6) in the proximal stent segment. The median stent expansion index was 0.77 (IQR 0.71-0.85). When assessed according to the underlying lesion morphology, indices of stent expansion did not significantly differ (Table 4).

### REGRESSION ANALYSIS

Table 5 contains key lesion and procedural variables that were selected for logistic regression analysis to identify characteristics that predict a greater than median stent elongation. The MSA achieved in the proximal segment and the category of lesion morphology were significantly associated with a greater than median relative stent elongation from univariable analysis. When incorporated into a multivariable model, the category of plaque morphology, specifically the presence of a lipid-rich plaque, remained significantly predictive of a greater than median percentage stent elongation, with an OR of 3.689 (95% CI: 1.604-8.484) relative to fibrocalcific plaque ( $p=0.002$ ). The MSA achieved in the proximal segment ceased to be significantly predictive of longitudinal stent behaviour, suggesting that any effect was, at least in part, mediated by the associated plaque morphology.

### Discussion

In this study, we present the largest analysis of *in vivo* longitudinal stent behaviour, as assessed by intracoronary OCT, and the first study to assess the impact of morphological characteristics of coronary plaque on DES elongation following implantation and optimisation during PCI to bifurcation lesions. We show that, following PCI, the relative stent length increased by 4.4% (IQR 1.0-8.9) across all lesions, with an absolute increase of 1.3 mm (IQR 0.3-2.2). Our study indicates that plaque morphology may be an

important mediator of the degree of stent elongation, which is a novel finding and of significant clinical importance.

DES are increasingly used in the treatment of advanced and complex patterns of coronary artery disease, characterised by multivessel interventions, longer lesion length and more challenging lesion morphologies, such as fibrotic plaque or heavy calcification<sup>22</sup>. To mitigate these challenges, stent platforms have evolved to provide high radial mechanical strength and reliable deliverability. However, the impact of these changes on the longitudinal biomechanical properties of contemporary stent platforms is less clear, with reduced longitudinal strength raising the risk of deformation and post-expansion elongation, both of which have significant potential procedural implications.

Early observations with contemporary DES suggested that improved deliverability may have come at the expense of longitudinal strength, with reports of stent compression and significant shortening both *in silico* and *in vivo*<sup>23,24</sup>. However, in 210 successive patients treated with 233 second-generation DES, a relative stent elongation of 5.24% (IQR 2.55-8.29) from baseline was reported, as assessed by intravascular ultrasound (IVUS). This equated to a median absolute increase in stent length of 0.90 mm (IQR 0.48-1.39), which was deemed not to be clinically important<sup>25</sup>.

In the treatment of bifurcation lesions, proximal optimisation involves the overexpansion of the stent in the main branch proximal to the carina, in order to ensure adequate expansion and apposition<sup>26</sup>. Recent observations, both *in silico* and *in vivo* in 36 patients assessed with intracoronary OCT, demonstrated significant stent elongation following POT<sup>8,9</sup>. Toth et al demonstrated a mean absolute stent elongation of 2.22±1.35 mm, and a relative elongation of 9.53±7.24%. *In vivo* there was no relationship between the tertile of overexpansion and the degree of elongation<sup>9</sup>.

In our study, we observed significant stent elongation following optimisation of PCI *in vivo*, with the degree of absolute and relative stent elongation in keeping with

**Table 5. Regression analysis to identify predictors of a greater than median increase in stent length from the nominal baseline length.**

	Univariable odds ratio (95% CI)	<i>p</i> -value	Multivariable odds ratio (95% CI)	<i>p</i> -value
<b>Lesion characteristics</b>				
Left main bifurcation	0.774 (0.360-1.723)	0.526		
Any major bifurcation (SB diameter ≥2.75 mm)	1.129 (0.533-2.391)	0.751		
Minimum lumen area, mm <sup>2</sup>	0.931 (0.620-1.400)	0.733		
Plaque morphology category (vs fibrocalcific)		0.002		0.007
Fibrous plaque	0.741 (0.136-4.031)	0.728	1.121 (0.238-5.269)	0.885
Lipid-rich plaque	3.951 (1.772-8.808)	<0.001	3.689 (1.604-8.484)	0.002
<b>Procedural characteristics</b>				
Final kissing balloon inflation	5.250 (0.568-48.496)	0.144		
Post-dilatation/POT balloon overexpansion, %	1.017 (0.989-1.046)	0.230		
Achieved MSA	1.074 (0.917-1.258)	0.378		
Proximal segment only	1.197 (1.021-1.402)	0.026	1.168 (0.989-1.379)	0.068
Distal segment only	1.067 (0.923-1.234)	0.378		
Achieved relative stent expansion	0.992 (0.975-1.008)	0.328		
Proximal segment only	1.002 (0.980-1.025)	0.833		
Distal segment only	0.988 (0.959-1.018)	0.445		
Achieved SEI	1.007 (0.973-1.042)	0.698		
Proximal segment only	1.009 (0.981-1.038)	0.521		
Distal segment only	1.001 (0.966-1.036)	0.965		

P-values in bold indicate statistical significance. CI: confidence interval; MSA: minimum stent area; POT: proximal optimisation technique; SB: side branch; SEI: stent expansion index

previous reports<sup>9,25</sup>. Improved performance of second- and third-generation DES in complex patterns of disease have resulted in contemporary trends for implanting longer lengths of stents. With a 48 mm long stent platform, a relative elongation of 6.4% (as seen with lipid-rich plaque) would result in absolute stent elongation of up to 3.1 mm. In this era of “precision PCI”, an unanticipated stent elongation of this magnitude could potentially result in clinically meaningful and unacceptable consequences, including major underexpansion and malapposition of the stent inflow, unintended protrusion of the stent from the coronary ostia, or unexpected coverage of proximal side branch ostia (**Central illustration**).

The mechanisms behind stent elongation are unclear and may reflect the modifications in stent structure of contemporary platforms that prioritise deliverability over longitudinal strength, including thinner struts, and fewer connectors between struts<sup>5,23</sup>. Previous studies proposed that stent elongation is most pronounced when an arc of malapposed stent struts exceeds 180° and the shoulders of the post-dilatation balloon abut the carina during POT. As the balloon expands, it is proposed that the shoulders of the balloon expand into the distal vessel segment ostium, and the balloon is consequently forced backwards, placing a longitudinal traction on malapposed stent struts. *In silico*, this may cause elongation of between 5-10%<sup>7,9</sup>.

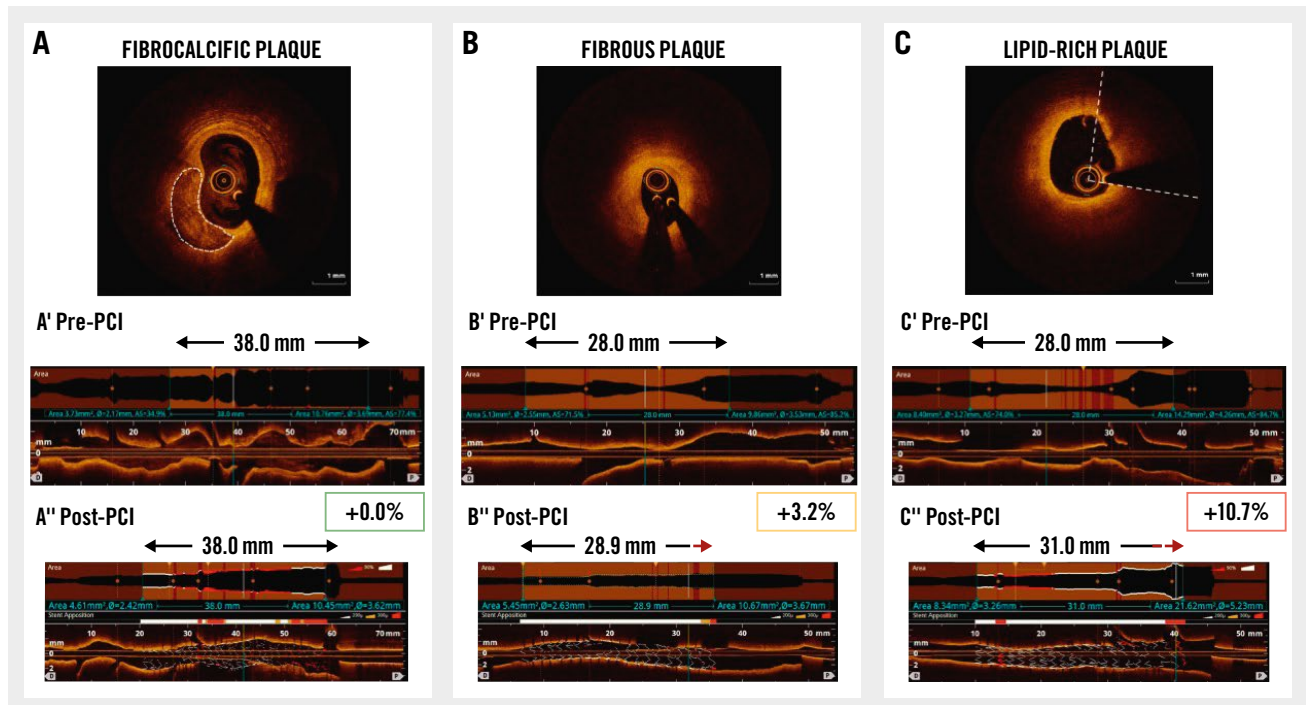
An important novel finding in our cohort is that the degree of stent elongation is, at least in part, mediated by the underlying plaque morphology. Our observations demonstrate that lipid-rich plaque facilitates stent elongation

of 6.4% (IQR 3.1-11.1). In fibrocalcific disease, however, the inherent vascular rigidity that is known to attenuate radial stent expansion may also apply a longitudinal traction that resists stent elongation.

In this study, we report various measures of absolute and relative stent expansion. Despite compelling *in silico* data relating DES overexpansion to elongation, these candidate variables were not predictive of elongation in our “real-world” cohort. These findings are in agreement with the *in vivo* findings of Toth et al and suggest that plaque morphology, determined by OCT, may be of greater importance in predicting elongation *in vivo*<sup>9</sup>.

This study has several potentially important clinical implications. This study appears to confirm a tendency of contemporary DES to elongate during post-dilatation, a finding with relevance across the field of PCI. When treating ostial lesions, the precise placement of stent struts is essential, and an appreciation of underlying plaque morphology may be necessary to ensure optimal stent coverage and avoid protrusion of the stent from the coronary ostia. Of equal importance are bifurcation lesions or lesions in the midportion of the vessel where, even with judicious stent placement, backwards elongation may result in struts unintentionally covering a side branch ostium, obstructing future access and acting as a potential nidus for thrombus formation<sup>10</sup>. An appreciation of plaque morphology, assessed with intracoronary imaging, may now be viewed as a key step during PCI planning to anticipate *in vivo* stent behaviour and inform stent sizing and selection.

## Drug-eluting stents elongate during implantation – the magnitude of elongation is determined by the underlying plaque morphology.



Michael McGarvey *et al.* • *EuroIntervention* 2024;20:e1184-e1194 • DOI: 10.4244/EIJ-D-23-00663

Representative examples are shown for each plaque morphology: (A) fibrocalcific plaque, (B) fibrous plaque, and (C) lipid-rich plaque at baseline, with the pre-PCI identification of landing zones and required stent length (A', B', C'), and final stent length following implantation and post-dilatation (A'', B'', C''). Stent elongation by 3 mm in a lipid-rich plaque in the proximal LAD (C''). Following post-dilatation, malapposed proximal struts lie across the ostium of the left circumflex. LAD: left anterior descending artery; PCI: percutaneous coronary intervention

### Limitations

This is a single-centre, retrospective study using intracoronary OCT to assess post-PCI stent length *in vivo*. While this enabled the collection of a rich dataset and a standardised protocol for OCT image analysis, it does introduce the possibility of bias.

We performed a qualitative analysis of lesion morphology, based on the predominant morphological characteristics at the site of minimum lumen area. Such an approach facilitates categorisation and comparison that can be practically applied in the catheterisation laboratory. OCT analysis demonstrated appropriate and significant differences in maximum lipid arc, lipid length, and calcium volume across groups. When validated by an independent OCT expert, our classification method proved reproducible with substantial agreement (Cohen's  $\kappa$  statistic of 0.71).

Despite this, we recognise that such an approach does not fully represent the heterogeneity of coronary atherosclerotic plaque. An analysis integrating a fully quantitative assessment of plaque composition may add further insight.

The choice of DES and interventional device was at the discretion of the treating clinician, with CoCr-EES used in over 60% of the cohort. CoCr-EES are amongst the most extensively validated of contemporary DES platforms, acting as the comparator arm in several randomised controlled trials<sup>27</sup>. We chose to limit the period of our study to between July 2017 and March 2022 in order to focus on second- and third-generation DES only, reflecting contemporary practice. This led to the exclusion of a number of patients, but, given the shared mechanical properties of second- and third-generation DES platforms, it is likely that our findings are generalisable<sup>4,5</sup>.

It is recognised that the use of IC imaging to guide PCI influences technique, resulting in the selection of longer stent lengths, and larger-diameter post-dilatation/POT balloons<sup>28</sup>. Stent overexpansion during post-dilatation/POT was not a predictor of stent elongation in our study, but *in silico* tests (which do not simulate the role of plaque morphology) suggest that elongation increases in proportion to balloon overexpansion<sup>9</sup>. It remains possible that the observed

stent elongation in this study is an artefact associated with the use of IC imaging and the subsequent selection of larger post-dilatation and POT balloons.

Due to the retrospective nature of our study, we are unable to reliably report the type of balloon used during post-dilatation (i.e., non-compliant vs compliant), the pressure applied during balloon inflation, or the sequence or number of balloon inflations. This has particular importance given recent *in silico* observations that a “modified” POT, initially optimising the stent inflow, may attenuate elongation<sup>29</sup>.

Patients were included in the study cohort if there was a baseline OCT assessment (prior to stent implantation) and a further assessment following stent placement and post-dilatation. In a minority of cases, there was further stent post-dilatation and optimisation, but a final OCT was not recorded.

Future prospective studies should include protocolised OCT assessment at each stage of the PCI procedure, including baseline assessment of morphology, with an assessment immediately following stent implant at nominal pressure, and a final assessment after completion of post-dilatation and POT. Performance of an OCT assessment prior to post-dilatation would allow an assessment of whether elongation occurred during implantation or during post-dilatation – using fiducial landmarks to assess if the elongation is symmetrical across the stent length or asymmetrical, predominantly affecting portions undergoing greater relative overexpansion. Such prospective analysis would also facilitate the evaluation of the clinical significance of this phenomenon.

Finally, the use of IC imaging to assess changes in stent length *in vivo* may itself introduce error. Our technique for the measurement of stent length has not been validated with histology studies, which remain the “gold standard”. Artefacts due to cardiac motion, the cyclic change of bifurcation angles during systole/diastole<sup>30</sup>, or wire bias due to the natural curvature of coronary arteries are possible. This may result in artefactual lengthening (or shortening) of the apparent stent length, depending on the vessel geometry and reflection of the near-infrared light signal. We attempted to minimise any potential impact of this by selecting only interventions in the left main and left anterior descending arteries, which usually have less tortuosity or curvature. Whilst we believe this allowed us to focus on the longitudinal behaviour of the stent and the impact of POT, future studies should assess whether our observations are conserved across all bifurcation and non-bifurcation lesions.

## Conclusions

Contemporary drug-eluting stents elongate during implantation and post-dilatation, an effect which is mediated by plaque morphology. This is an important consideration when assessing plaque morphology, planning strategy, selecting interventional devices and assessing results immediately following DES optimisation.

## Authors' affiliations

1. Department of Cardiology, King's College Hospital NHS Foundation Trust, London, United Kingdom; 2. School of Cardiovascular and Metabolic Medicine & Sciences, BHF Centre of Excellence, King's College London, London, United Kingdom; 3. Bristol Heart Institute, University Hospitals

Bristol NHSFT & University of Bristol, Bristol, United Kingdom; 4. Royal Free NHS Foundation Trust, London, United Kingdom; 5. Department of Cardiology, Royal Brompton & Harefield Hospitals, Guy's & St Thomas' NHS Foundation Trust, London, United Kingdom

## Funding

This work was part-funded by King's College Hospital R&D Grant and was supported by the Department of Health via a National Institute for Health Research Biomedical Research Centre award to Guy's & St Thomas' NHS Foundation Trust in partnership with King's College London and King's College Hospital NHS Foundation Trust.

## Conflict of interest statement

J.M. Hill has received honoraria, speaker fees and research grant support from Abbott, Abiomed, Boston Scientific, and Shockwave Medical; and has held equity in Shockwave Medical. T.W. Johnson has received personal fees from Abbott, Boston Scientific, Medtronic, and Terumo. N. Pareek has received speaker fees from Abbott. A.M. Shah is supported by the British Heart Foundation. The other authors have no conflicts of interest to declare.

## References

- Vaduganathan M, Mensah GA, Turco JV, Fuster V, Roth GA. The Global Burden of Cardiovascular Diseases and Risk: A Compass for Future Health. *J Am Coll Cardiol*. 2022;80:2361-71.
- Neumann FJ, Sousa-Uva M, Ahlsson A, Alfonso F, Banning AP, Benedetto U, Byrne RA, Collet JP, Falk V, Head SJ, Juni P, Kastrati A, Koller A, Kristensen SD, Niebauer J, Richter DJ, Seferović PM, Sibbing D, Stefanini GG, Windecker S, Yadav R, Zembala MO. 2018 ESC/EACTS Guidelines on myocardial revascularization. *EuroIntervention*. 2019;14:1435-534.
- Stefanini GG, Alfonso F, Barbato E, Byrne RA, Capodanno D, Colleran R, Escaned J, Giacoppo D, Kunadian V, Lansky A, Mehilli J, Neumann FJ, Regazzoli D, Sanz-Sanchez J, Wijns W, Baumbach A. Management of myocardial revascularisation failure: an expert consensus document of the EAPCI. *EuroIntervention*. 2020;16:e875-90.
- Ng J, Foin N, Ang HY, Fam JM, Sen S, Nijjer S, Petraco R, Di Mario C, Davies J, Wong P. Over-expansion capacity and stent design model: An update with contemporary DES platforms. *Int J Cardiol*. 2016;221:171-9.
- Watson T, Webster MWI, Ormiston JA, Ruygrok PN, Stewart JT. Long and short of optimal stent design. *Open Heart*. 2017;4:e000680.
- Eeckhout E, Kappenberger L, Goy JL. Stents for intracoronary placement: current status and future directions. *J Am Coll Cardiol*. 1996;27:757-65.
- Matsuda Y, Ashikaga T, Sasaoka T, Hatano Y, Umemoto T, Yamamoto T, Maejima Y, Hirao K. Effectiveness of the proximal optimization technique for longitudinal stent elongation caused by post-balloon dilatation. *J Interv Cardiol*. 2018;31:624-31.
- Sumi T, Ishii H, Tanaka A, Suzuki S, Kojima H, Iwakawa N, Aoki T, Hirayama K, Mitsuda T, Harada K, Negishi Y, Ota T, Kada K, Murohara T. Impact of post-dilatation on longitudinal stent elongation: An in vitro study. *J Cardiol*. 2018;71:464-70.
- Toth GG, Achim A, Kafka M, Wu X, Lunardi M, Biswas S, Shahzad A, Thury A, Ruzsa Z, Johnson TW, Wijns W. Bench test and in vivo evaluation of longitudinal stent deformation during proximal optimisation. *EuroIntervention*. 2022;18:83-90.
- Paradies V, Lu S, Ng J, Ang HY, Joner M, Foin N. Thrombogenicity at the jailed side branch ostia in the provisional stenting technique: insights from an in vitro model. *EuroIntervention*. 2018;14:826-7.
- Fujino A, Mintz GS, Matsumura M, Lee T, Kim SY, Hoshino M, Usui E, Yonetsu T, Haag ES, Shlofmitz RA, Kakuta T, Maehara A. A new optical

coherence tomography-based calcium scoring system to predict stent underexpansion. *EuroIntervention*. 2018;13:e2182-9.

12. Lunardi M, Louvard Y, Lefevre T, Stankovic G, Burzotta F, Kassab GS, Lassen JF, Darremont O, Garg S, Koo BK, Holm NR, Johnson TW, Pan M, Chatzizisis YS, Banning A, Chieffo A, Dudek D, Hildick-Smith D, Garot J, Henry TD, Dangas G, Stone GW, Krucoff MW, Cutlip D, Mehran R, Wijns W, Sharif F, Serruys PW, Onuma Y; Bifurcation Academic Research Consortium and European Bifurcation Club. Definitions and Standardized Endpoints for Treatment of Coronary Bifurcations. *J Am Coll Cardiol*. 2022;80:63-88.
13. (NICOR) NioCOR. National Audit of Percutaneous Coronary Intervention (NAPCI): 2023 Summary Report 2023. Available from : <https://www.nicor.org.uk/national-cardiac-audit-programme/previous-reports/pci-1/2023-5/10633-nicor-annual-summary-reports-napci-v5-ac?layout=default>. (Last accessed: 25 July 2024).
14. Tearney GJ, Regar E, Akasaka T, Adriaenssens T, Barlis P, Bezerra HG, Bouma B, Bruining N, Cho JM, Chowdhary S, Costa MA, de Silva R, Dijkstra J, Di Mario C, Dudek D, Falk E, Feldman MD, Fitzgerald P, Garcia-Garcia HM, Gonzalo N, Granada JF, Guagliumi G, Holm NR, Honda Y, Ikeno F, Kawasaki M, Kochman J, Koltowski L, Kubo T, Kume T, Kyono H, Lam CC, Lamouche G, Lee DP, Leon MB, Maehara A, Manfrini O, Mintz GS, Mizuno K, Morel MA, Nadkarni S, Okura H, Otake H, Pietrasik A, Prati F, Räber L, Radu MD, Rieber J, Riga M, Rollins A, Rosenberg M, Sirbu V, Serruys PW, Shimada K, Shinke T, Shite J, Siegel E, Sonoda S, Suter M, Takarada S, Tanaka A, Terashima M, Thim T, Uemura S, Ughi GJ, van Beusekom HM, van der Steen AF, van Es GA, van Soest G, Virmani R, Waxman S, Weissman NJ, Weisz G; International Working Group for Intravascular Optical Coherence Tomography (IWG-IVOC). Consensus standards for acquisition, measurement, and reporting of intravascular optical coherence tomography studies: a report from the International Working Group for Intravascular Optical Coherence Tomography Standardization and Validation. *J Am Coll Cardiol*. 2012;59:1058-72.
15. Kini AS, Vengrenyuk Y, Shameer K, Maehara A, Purushothaman M, Yoshimura T, Matsumura M, Aquino M, Haider N, Johnson KW, Readhead B, Kidd BA, Feig JE, Krishnan P, Sweeny J, Milind M, Moreno P, Mehran R, Kovacic JC, Baber U, Dudley JT, Narula J, Sharma S. Intracoronary Imaging, Cholesterol Efflux, and Transcriptomes After Intensive Statin Treatment: The YELLOW II Study. *J Am Coll Cardiol*. 2017;69:628-40.
16. Räber L, Mintz GS, Koskinas KC, Johnson TW, Holm NR, Onuma Y, Radu MD, Joner M, Yu B, Jia H, Meneveau N, de la Torre Hernandez JM, Escaned J, Hill J, Prati F, Colombo A, di Mario C, Regar E, Capodanno D, Wijns W, Byrne RA, Guagliumi G; ESC Scientific Document Group. Clinical use of intracoronary imaging. Part 1: guidance and optimization of coronary interventions. An expert consensus document of the European Association of Percutaneous Cardiovascular Interventions. *Eur Heart J*. 2018;39:3281-300.
17. Ali Z, Landmesser U, Karimi Galougahi K, Maehara A, Matsumura M, Shlofmitz RA, Guagliumi G, Price MJ, Hill JM, Akasaka T, Prati F, Bezerra HG, Wijns W, Mintz GS, Ben-Yehuda O, McGreevy RJ, Zhang Z, Rapoza RR, West NEJ, Stone GW. Optical coherence tomography-guided coronary stent implantation compared to angiography: a multicentre randomised trial in PCI - design and rationale of ILUMIEN IV: OPTIMAL PCI. *EuroIntervention*. 2021;16:1092-9.
18. Rai H, Harzer F, Otsuka T, Abdelwahed YS, Antuña P, Blachutzik F, Koppa T, Räber L, Leistner DM, Alfonso F, Nef H, Seguchi M, Aytekin A, Xhepa E, Kufner S, Cassese S, Laugwitz KL, Byrne RA, Kastrati A, Joner M. Stent Optimization Using Optical Coherence Tomography and Its Prognostic Implications After Percutaneous Coronary Intervention. *J Am Heart Assoc*. 2022;11:e023493.
19. He H, Ma Y, editors. Imbalanced learning: foundations, algorithms, and applications. The Institute of Electrical and Electronics Engineers, Inc. 2013.
20. Altman DG, Royston P. The cost of dichotomising continuous variables. *BMJ*. 2006;332:1080.
21. Landis JR, Koch GG. The measurement of observer agreement for categorical data. *Biometrics*. 1977;33:159-74.
22. Serruys PW, Ono M, Garg S, Hara H, Kawashima H, Pompilio G, Andreini D, Holmes DR Jr, Onuma Y, King Iii SB. Percutaneous Coronary Revascularization: JACC Historical Breakthroughs in Perspective. *J Am Coll Cardiol*. 2021;78:384-407.
23. Ormiston JA, Webber B, Webster MW. Stent longitudinal integrity bench insights into a clinical problem. *JACC Cardiovasc Interv*. 2011;4:1310-7.
24. Rhee TM, Park KW, Lee JM, Lee MS, Jeon KH, Kang HJ, Koo BK, Rhew JY, Cha KS, Bae JH, Han KR, Park SH, Park WJ, Rha SW, Oh SK, Kwon HM, Seung KB, Ahn T, Kim SH, Kim HS. Predictors and Long-Term Clinical Outcome of Longitudinal Stent Deformation: Insights From Pooled Analysis of Korean Multicenter Drug-Eluting Stent Cohort. *Circ Cardiovasc Interv*. 2017;10:e005518.
25. Dvir D, Kitabata H, Barbash IM, Minha S, Badr S, Loh JP, Chen F, Torguson R, Waksman R. In vivo evaluation of axial integrity of coronary stents using intravascular ultrasound: Insights on longitudinal stent deformation. *Catheter Cardiovasc Interv*. 2014;84:397-405.
26. Finet G, Derimay F, Motreff P, Guerin P, Pilet P, Ohayon J, Darremont O, Rioufol G. Comparative Analysis of Sequential Proximal Optimizing Technique Versus Kissing Balloon Inflation Technique in Provisional Bifurcation Stenting: Fractal Coronary Bifurcation Bench Test. *JACC Cardiovasc Interv*. 2015;8:1308-17.
27. Bangalore S, Toklu B, Patel N, Feit F, Stone GW. Newer-Generation Ultrathin Strut Drug-Eluting Stents Versus Older Second-Generation Thicker Strut Drug-Eluting Stents for Coronary Artery Disease. *Circulation*. 2018;138:2216-26.
28. Ali ZA, Maehara A, Généreux P, Shlofmitz RA, Fabbicocchi F, Nazif TM, Guagliumi G, Meraj PM, Alfonso F, Samady H, Akasaka T, Carlson EB, Leesar MA, Matsumura M, Ozan MO, Mintz GS, Ben-Yehuda O, Stone GW; ILUMIEN III: OPTIMIZE PCI Investigators. Optical coherence tomography compared with intravascular ultrasound and with angiography to guide coronary stent implantation (ILUMIEN III: OPTIMIZE PCI): a randomised controlled trial. *Lancet*. 2016;388:2618-28.
29. Gupta H, Kaur N, Revaiah PC. Modified proximal optimisation technique for long left main interventions to prevent stent elongation. *AsiaIntervention*. 2024;10:38-9.
30. Wang Z, Yang J, Li C, Huang J, Fezzi S, Chen E, Cai W, Stankovic G, Wijns W, Chen L, Tu S. Dynamic assessment of the left main-left circumflex bending angle: Implications for ostial left circumflex artery in-stent restenosis after successful two-stent PCI. *Int J Cardiol*. 2023;378:11-19.